Spatial confinement: A spur for axonal growth

Catherine Villard

Spatial confinement: a spur for axonal growth

Catherine Villard

Laboratoire Interdisciplinaire des Energies de Demain (LIED),
Université Paris Cité, UMR 8236 CNRS, F-75013, Paris, France
E-mail: catherine.villard@u-paris.fr.

Keywords: growth cone, velocity, micropatterns, topography, confinement

Abstract
The concept of spatial confinement is the basis of cell positioning and guidance in in vitro studies. In vivo, it reflects many situations faced during embryonic development. In vitro, spatial confinement of neurons is achieved using different technological approaches: adhesive patterning, topographical structuring, microfluidics and the use of hydrogels. The notion of chemical or physical frontiers is particularly central to the behaviors of growth cones and neuronal processes under confinement. They encompass phenomena of cell spreading, boundary crossing, and path finding on surfaces with different adhesive properties. However, the most universal phenomenon related to confinement, regardless of how it is implemented, is the acceleration of neuronal growth. Overall, a bi-directional causal link emerges between the shape of the growth cone and neuronal elongation dynamics, both in vivo and in vitro. The sensing of adhesion discontinuities by filopodia and the subsequent spatial redistribution and size adaptation of these actin-rich filaments seem critical for the growth rate in conditions in which adhesive contacts and actin-associated clutching forces dominate. On the other hand, the involvement of microtubules, specifically demonstrated in 3D hydrogel environments and leading to ameboid- like locomotion, could be relevant in a wider range of growth situations. This review brings together a literature collected in distinct scientific fields such as development, mechanobiology and bioengineering that highlight the consequences of confinement and raise new questions at different cellular scales. Its ambition is to stimulate new research that could lead to a better understanding of what gives neurons their ability to establish and regulate their exceptional size.

1 – Introduction

Brain tissues and dissociated neurons in culture dishes represent diametrically opposed systems on the complexity scale. Between these two extremes, technological approaches of structuring substrates, both at the chemical and topographical levels, allow the in vitro imple- mentation of specific characteristics or functions of cells and organs. These approaches emerged in the 90's with the development of micropatterning technologies (see [1] for a history in the particular case of neuroscience). They rapidly led to the control of single cell geometry, as illustrated by the seminal work of Chen et al. about the link between cell size and cell viability [2]. In addition, for neurosciences where the notion of cellular network is crucial, these technologies have led to the in vitro implementation of neuronal microcircuits. This has occurred almost concomitantly using micropatterning [3] and microfluidic techniques [4]. In both approaches, the aim is to position the soma and to guide the growth of their extensions, mostly axons.
In these positioning and guidance strategies lies the notion of cellular confinement. Indeed, a single neuron forming autapses inside an adhesive circle [5], a neuronal process (neurite) guided by a thin stripe [6], or a soma constrained by a boomerang shape [7] are confined by the limits of adhesive patterns. Similarly, an axon guided by a microfluidic channel whose lateral dimensions are smaller than that of its growth cone (GC) will be confined in both width and height.

This review is dedicated to how neurons, and their main sub-cellular compartments that are GCs and neurites, respond to a spatial confinement. Although I will heavily rely on in vitro micro-engineering approaches in this work, I would like to state that cellular growth in confined situations is not only a technological mean and the cell behavior under confinement an unavoidable contingency of in vitro systems. Importantly, neuronal growth occurs during the embryonic stage in a crowded non-homogeneous physico-chemical environment. Therefore, confinement is also a physical cue encountered in the developing nervous system. The developing cortex gives a paradigmatic example of neuron navigation in a packed tissue. The inside-out birth order arrangement of neurons imposes their progenitors to migrate from the sub-plate to the pial surface i.e., from the deepest (and more and more populated as embryonic time passes) to the upper layers of the cortex along the thin processes of radial glia [**8**]. Another example in the same line concerns follower axons growing on pioneer axons which provide them with a scaffold [**9**]. A micron-size adhesive stripe, a fiber or a microchannel, all situations implementing confinement in vitro would be a much better model of these in vivo conditions than the bottom surface of a Petri dish.
Besides, in vitro technologies provides exquisite control over the chemical and physical microenvironment at the micron scale, allowing to echo more faithfully in vivo situations than conventional 2D cultures and, even more interestingly, to reveal behaviors otherwise kept hidden (see [**10**] for a discussion on these aspects).

Cytoskeletal organization and dynamics as well as biomechanical aspects of neuronal growth are central to the response of neurons to confinement. Regarding specifically GCs, the reader can refer to recent reviews focusing on actin-based [**11**] and microtubule-based [**12**] mechanisms underlying GC motility, as well as on the crosstalk between both types of filaments [**13, 14**]. These reviews consider implicitly neurons evolving on 2D surfaces. In such a situation, GCs are compartmentalized into three zones dominated by the presence of one type of cytoskeletal structure: microtubules emerging from the shaft in the *central* zone hitting an acto-myosin arc (defining the *transition* zone) beyond which the actin-rich *peripheral* domain extends [**15**]. The existence of an actin-microtubule crosstalk, supported by multiple microtubule-associated proteins (MAPs) (see [**12**] for a review), somehow blurs this stereotypical structural view, leading through different proposed mechanistic scenarios to microtubule invasion of the peripheral domain, controlling the distribution of filopodia length and lifetime along the GC perimeter.
Basically and importantly, both cytoskeleton filaments can sense or apply mechanical forces, from their interaction with the local microenvironment trough adhesion complexes.
The currently accepted mechanical view of neuronal growth is that the endogenous forces exerted by the GC are dissipated by adhesions along visco-elastic neurites [**16**, **17**, **18**]. In addition, neurites display an active i.e., contractile behavior [**19**, **20**, **21**, **22**,**23**]. A dynamic imbalance between the shaft contractility and the traction forces produced by the GC may govern the elongation rate. As an illustration of this conceptual framework, it was reported that diffusing and surface-bound repellents increase the relative part of the contractile contribution, while forward growth could be then restored by the inhibition of key molecular pathways responsible of cell contractility [**24**]. The readers can refer to [**25**] for an illuminating review about how mechanics couples with the chemical environment of neurons. How these acto-myosin mediated contractile forces are produced at the molecular level is not currently fully understood, but stems from the existence of actin rings arranged perpendicularly to the axon axis, spaced by spectrin tetramers and connected to myosin II motors [**26**] [**27**]. Several mechanical models takes into account the interplay of GC pushing and pulling forces, shaft viscoelasticity and contractility, and adhesions to describe axonal elongation (see, e.g. the detailed review of Olivery and Goriely [**28**]). Lastly, a complete picture of the mechanical link between the soma and the GC should include GC-like, anterogradely propagative structures produced in extending mammalian neurons [**29**, **30**]. It was proposed that these so-called actin waves might extend the mechanical range of action of the GC during the neuron elongation phase, in addition to their contribution to slow transport [**31**].

Note that the mechanisms discussed above concern the existence of a GC seeking for a target. But, as stated in Rossi et al., "axons that already reached their targets have to elongate further to match the progressive expansion of the nervous system or of the whole organism" [32]. This interstitial growth modality is another evidence of axonal visco-elastic properties (for a review about interstitial growth, see [33]) and of force-mediated mass generation in the shaft [34].

The present review will cover the various approaches of different origins (chemical, physical) leading to the implementation of a confinement: adhesive patterns, topographies that are close enough to force neuronal extensions to squeeze between them, and hydrogels providing resistive forces distributed allover the surface of the cell.
Confinement means frontiers or spatial borders. I will review in a first chapter the phenomenon of morphological adaptation to adhesive areas delimited by frontiers with less permissive surfaces. These phenomena give rise to an unexpected wealth of cellular responses supported by a competition between an affinity for sharp adhesion gradients and a limited spread capacity on adhesive surfaces. Once explored the modalities of interaction with frontiers, I will discuss under what conditions and how neurons cross these boundaries to reach nearby adhesive zones by passing over surfaces less favorable to cell adhesion.
The core part of this review (section 3) describes the generic behavior of enhanced growth rate under confinement, whatever the chemical or physical nature of this confinement. The strategies of confinement will be sorted by their dimensionality and practical modalities of implementation.
The next section will give some mechanistic clues about the responses to confinement, focusing on the sensing mechanisms of filopodia. Interestingly, confinement provides either restrictions or incentives in filopodia extension, and finally tunes the balance between both. This section also highlights several possible analogies between neuronal and non-neuronal cells, which may help decipher, from the vast literature of migration mediated by pulling or pushing forces, the molecular mechanisms at work in neuronal growth in confined situations.
I will finally discuss in section 5 the link between GC morphology and their dynamics both in vitro and in vivo.
This review will end with a list of open questions regarding cell spreading mechanisms on finite size adhesive areas and growth acceleration under spatial confinement.

2 – Neuron response to differential adhesive properties

Neurons respond to chemical cues presented on a substrate by adapting their morphology and growth dynamics. I will consider here the case of a composite substrate composed of contiguous surfaces presenting a contrast of adhesive properties. These surfaces thus define frontiers characterized by sharp adhesive gradients. In the simplest case of only two different surface chemistry, e.g., adhesive areas on a less permissive background, I can define two situations depending on the geometry and spatial distribution of these frontiers: (i) they delimits small, enclosed adhesive surfaces isolated from each other, or (ii) they come close enough to form a network of adhesive areas. Note that the concepts of "small" or "close" have to be considered from the point of view of neurons, in other terms compared to the size or the exploratory abilities of their main sub-cellular compartments.
The two situations defined above can be associated with adaptive behaviors described as (i) morphological adaptation to the shape of adhesive surfaces, (ii) crossing-associated behaviors, and (iii) guidance by frontiers. I review in the three following sections a few highlights from the literature dedicated to these behaviors.
I will consider here both GCs, the dynamic structures located at the tip, and neurites. The spatio-temporal dynamics of GCs and their overall shapes determine neurite growth rate. Note that the reverse proposition is also true: environmental conditions may affect neurite growth and this may in turn tune the shape of GCs (this aspect will be treated in section 5).

2.1. Morphological adaptive responses to enclosed adhesive surfaces

It is well established, both in vivo and in vitro, that the size of a GC varies with the molecular composition or topography of its environment. Here I examine situations where GCs modulate their size and shape in response to adhesive confinement. Generally speaking they can spread when encountering closed surfaces of optimal size. Neurites behave in a similar manner, although this aspect has been less documented in vitro, and even less in vivo. Interestingly, this adaptive behavior to confinement includes the mirror phenomenon of "de-spreading" that occurs when the boundaries delimiting the adhesive surfaces move apart, as described below.

2.1.1. Growth cone size adaptation to adhesive surfaces

In an earlier work, Clark et al. reported that GCs of mice dorsal root ganglion neurons adopt a tapered morphology on 6µm wide stripes, make contact with both borders of 12 µm wide stripes but only manage to keep contact with a single border of 25 µm lines, being unable to span across the full width of the largest adhesive stripe [6]. Such observation is quite generic for many neuronal types (see an example in figure 1a for mice cerebellar granule neurons).

More generally, there is a competition between the affinity of GCs for sharp adhesive gradients, leading them to spread in order to make contact with adhesive frontiers, and their limited capacity of spreading. This competition triggers a wealth of adaptive behaviors, described in a body of work using e.g., laminin spots deposited on a PLL background [35], PLL discs surrounded by IK [36] or semaphorin 3F [37] (figure 1b-c). Smirnov et al. [38] and Liu et al. [39] observed a similar phenomenon when GCs confined into narrow adhesive stripes enter a node or a larger surface of spreading, respectively.

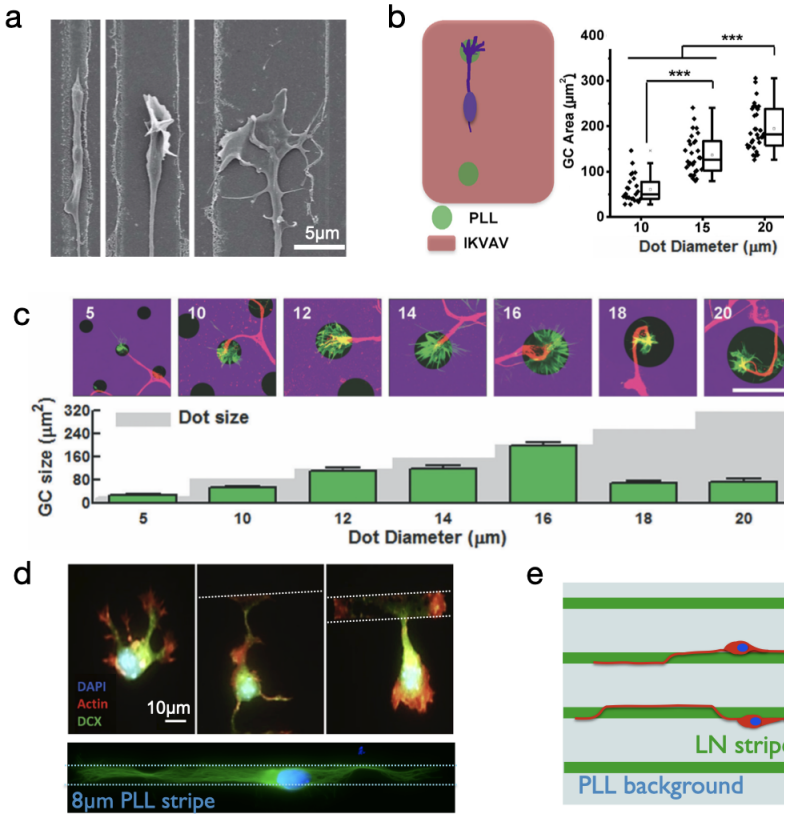

Figure 1 – Perception of sharp change of adhesive molecule concentrations
A-C: Perception of frontiers by growth cones (GCs). A-GC spreading on laminin (LN) stripes deposited on a polyvinyl alcohol background. Adapted with permission from Smirnov et al. (2014) [38]. B–Scheme and quantification of GC size on PLL dots on IKVAV (a 19- mer laminin peptidomimetic) background. Adapted with permission from Zhao et al. (2019) [36]. C-Representative images and quantification of GC size of phalloidin-stained neurons on PLL dots of various diameters on a semaphorin 3F background. Neurons were stained with Tuj1 antibody (magenta: MTs) and fluorescein-labeled phalloidin (green: actin). Scale bar: 30 µm. Reproduced with permission from Ryu et al. (2019) [37]. **D-E:** Perception of frontiers by neurites. D-Cortical neuron soma adhering to IKVAV background outgrow neurites until the tip of one process reaches a 10 µm wide PLL stripe (borders of the stripe indicated by white dotted lines) on which first GC and then neurite attach and spread (top). Adapted with permission from Zhao et al. (2019) [36]. Alternation of microtubule defasciculation and bundling on the branches of a mouse hippocampal neuron confined into a 8 µm PLL stripe. Nucleus (Hoecht, blue), microtubules (β3-tubulin, green). Adapted with permission from Tomba 2014 [56]. E-Neurites, more than soma, are guided by sharp adhesive contrasts. See [49].

Both Zhao et al. [36] and Ryu et al. [37], using adhesive PLL disks of increasing diameters, reported that the spreading surface of the GC tend to match those of the discs. Interestingly, this behavior has an immediate consequence on the success rate of soma translocation (ST) to PLL disks from an initial neuron positioning on the less adhesive surface [36]. This rate is a monotonous function of PLL areas, showing that the spreading area of the GC tunes the efficiency of ST. More generally, this phenomenon occurs as soon as an adhesive contrast is provided between the initial soma location

and the area targeted by the GC [40, 41]. Very interestingly, Ryu et al. [37] increased the diameters of PLL disks in a large range, from 5 to 20 µm, and observed, after an initial joined increase of both GC and PLL surfaces, a GC shrinking above a disk diameter of 16 µm. This surface defines somehow the upper threshold of full adhesive confinement. The area of the GC stabilizes then around 80 μm^2 inside increasing large PLL dots, a value close to the one measured inside 10 µm diameter disks.
In short, the competition between affinity for adhesion gradients and spreading ability modulate the final shape of cellular structures. A matching between the adhesive and cell areas occurs when cell affinity for boundaries prevails, while the cell can be considered as "deconfined" when its spreading capacities are exceeded.

2.1.2. Neurite width adaptation to adhesive surfaces

Similarly to GCs, neurites display a strong affinity to sharp adhesive frontiers. More specifically, they tend to expand laterally to make contact with these boundaries. Although the spontaneous neurite diameter is on the order of the micron, neurites can strikingly spread to cover the width of 8 µm [42, 43] or even 10 µm PLL stripes [36] (figure 1d top). Neurite spreading is associated with unbundled and disorganized microtubules [35, 44]. Interestingly, neurites seem to undergo dynamical remodeling of their microtubule cytoskeleton versus time and space: debundling is preferentially observed close to the neurite tip for long processes but tend to vanish upstream of the GC [35, 44]. Instabilities in neurite width are also observed on 8 µm wide stripes [43] (figure 1d bottom).

2.2. Positioning of soma and neurites at adhesion frontiers

Neurites can be guided at the junction between horizontal and a vertical surface [45, 46, 47] or by topographies through the phenomenon of contact guidance [48]. Similarly, they are guided by sharp changes of adhesiveness provided on flat surfaces through differential molecular coatings. Xing et al. [49] designed LN stripes on a PLL background and observed neurites growth at the edges of 5 µm wide LN stripes, a situation more frequent when the soma sits also on the edges (figure 1e). This effect fades progressively under the threshold value of LN concentration of 20 µg/mL, i.e., when the adhesive contrast is not longer sufficient. Joo et al. observed a similar behavior on PLL stripes stamped on a PLL background [50]. This guidance effect persists for line width up to 10 µm, then decrease for a width of 15 µm [50] and is modulated by the initial position of the soma with respect to the lines [49]. Note that in contrast with this parallel guidance, perpendicular neurite orientation with respect to a frontier between substrates of different properties, here the rigidity, was observed [51 Tomba2022]. Overall, these guidance effects appear poorly reliable and efficient but highlight the exquisite sensitivity of thin processes like neurites to adhesion frontiers.

2.3. Growth dynamics induced by changing microenvironments

Although GCs cannot progress on uniform non-adhesive surfaces, distributed adhesive areas on a less favorable or even anti-fouling background surprisingly do not prevent neurite growth. This claim is already, at least in part, supported by the numerous observations of the perpendicular contact guidance phenomenon, where neurites elongate perpendicularly to e.g., grooves or navigate from the top of one micro or nanopillar to another under discontinuous adhesion conditions ([48] for a review).
I detail here dynamical and morphological GC properties during their journey on weakly or non-permissive surfaces separating more favorable areas. Here GCs do not loose physical contact with their substrate but their impaired or modified adhesion trigger specific behaviors.
GCs explore non-fouling or cell-repellant surfaces on a limited spatial range over maximum distances of the order of 50 µm [7, 40, 44, 52, 53, 54]. Unexpectedly, the average velocity of dissociated dorsal root ganglion (DRG) neurons from chick embryos grown on array of LN stripes increases with the distance between stripes [52]. A similar effect was reported for axon collaterals of hippocampal neurons at 2DIV on PLL dots [44, figure 2a]. Ryu et al. [37] reported similar observations for rat hippocampal neurons seeded on a composite substrate formed by 10 µm diameter PLL dots on a Sema3F background. These authors observed an increase of average speed with increasing the inter-

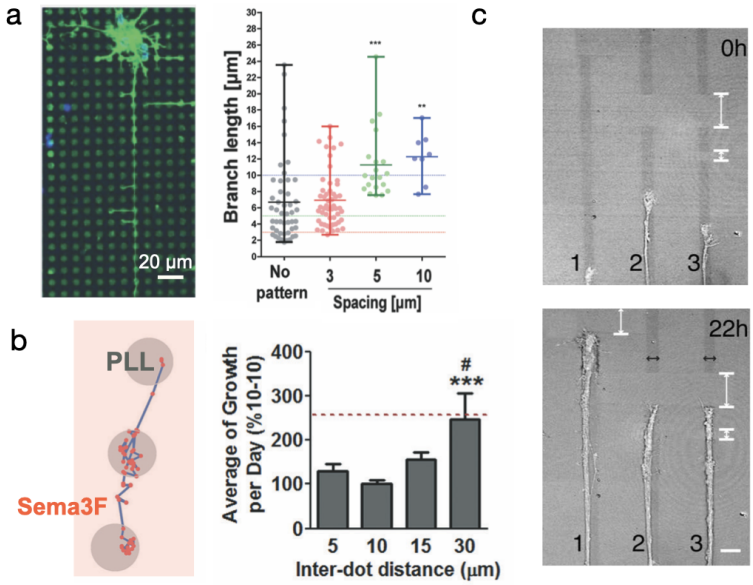

Figure 2 – Crossing dynamics
A-B: Growth velocity associated to crossing behavior between adhesive areas. A-Image of a branched neuron (microtubule β3-tubulin staining, green) on a Poly-D-lysine 5µm dot array. Graph: distribution of branch lengths on 3, 5 and 10 µm spaced dot arrays as compared to the no- pattern substrate at 2 DIV. Mean ± SEM,**p < 0.1, ***p < 0.001. Adapted with permission from Kim et al. (2014) [44]. B-Growth trajectory (scheme) and neurite outgrowth length (graph) over a 24-h time period as a function of the distance between 10 µm PLL disk stamped on a semaphorin 3F (Sema3F) background. Red dotted line indicated the values obtained from control neurons grown in absence of printed pattern. Length values are normalized to the values obtain-ned for a 10 µm distance between disks. Adapted with permission from Ryu et al. (2019) [37]. **C**–Axons elongating (22h time point interval) along 8 µm wide laminin stripes cross 10 µm non-adhesive gaps but stop at wider (i.e., 20 µm) gaps (indicated by white signs). Caliber of stopped axons increase as time passes. Scale bar: 12 µm. Adapted with permission from Turney et al. (2020) [54].

dot distance from 5 to 30 µm, reaching the value obtained from control neurons grown in absence of printed patterns (figure 2b). In addition, crossing the inter-dot Sema3F surface lead to GC instantaneous speed as high as 2.5 µm/min, more than an order of magnitude above the velocity on a homogeneous PLL or SemaF3 substrates, or on the dots themselves. This "slow down then go fast" of neurite growth appear to be generic, whatever the nature of the differential coatings implemented on the surfaces [35, 55]. Interestingly, neurites that do not succeed to cross a non-adhesive gap and whose growth is thus impeded tend to enlarge with time [54] (figure 2c), an observation supporting the concept of "growth pressure" proposed by [37].

3. Increase of growth velocity induced by confinement

I will consider here all types of confinement provided by engineered environments, sorting them by by confinement modalities and dimensionality. Remarkably, they all elicit an increased elongation velocity as compared to the unconfined situation expressed by a flat adhesive surface. This striking feature goes along other phenomena like a simplification of the neuronal geometry and neurite guidance. I review below a few highlights from the literature supporting this statement in this range of constrained microenvironements.

3.1. Lateral confinement

3.1.1. Adhesive constraints on flat substrates

The confinement imposed by adhesive stripes on flat substrates constrains the shape of GCs (figure 1a). It also induces an increase of the average growth velocity on adhesive stripes, assessed by the relative length of neuronal branches as compared to controls. This is the case for hippocampal embryonic rat neurons deposited on 3 µm PLL wide stripes stamped on a less concentrated PLL background: the length of the longest process at 2 days in vitro (DIV) is about twice the value of both the control (PLL background) and 15 µm PLL wide stripes (130 µm versus 70 µm) [50]. These results confirm those of [56] obtained on 2 to 8 µm wide PLL stripes using hippocampal embryonic mice neurons (figure 3a). This increase of length might be a combination of two effects: the reduction in the number of neurites, as neurons can protrude only two diametrically opposed branches on thin lines, and/or an increased intrinsic growth velocity. Subsequent work by Tomba et al. using 2, 3 and 4 branch patterns [43] has evaluated the contribution of these two factors and has concluded to a conservation of the total neurite length at 2 DIV independently of the numbers of branches. The conclusion of this study is that neuron length is tuned by the frequency of actin waves production and the increment of elongation they induce, both properties controlled by the proximal and distal

neurite width. Increase of the neurite length induced by widening the adhesive stripes width from 5 to 10 µm is also effective for SH-SY5Y differentiated cells (figure 3b) [57]. Beyond these systematic studies, among the fastest neurite average growth were reported for 2 µm wide stripes (i.e., 0.6 µm/min [40] as compared to the ~0.03 µm/min reported for the longest neurite on 2D PLL substrates [58 Sun, 59 Santos]). A discordant note comes however from the work of Smirnov et al., which reports no difference in the overall rate of GC advance on adhesive stripes in the range 1.5-12 µm for postnatal mice cerebellar granule neurons [38].

3.1.2. Topographical constraints

An extensive literature discussing contact guidance supports an enhanced global velocity when neurites are constrained by topographies (see [48] for a review, and e.g., [60] [61] for recent works on soft structured surfaces). The effect exists both on continuous structures like groves or on what could be described as dotted containment provided by pillared surfaces. This effect is all the more important as the pillar spacing is close to the neurite size [62] (figure 3c). A recent work of Milos et al. [63] addressed the issue of the dynamics of the typical growth phases of elongation, pausing and retraction on pillared surfaces. These structured substrates made of 500nm to 1 µm diameter posts (with a height of up to 400 nm) separated by an edge-to-edge distance equal to their diameter were designed to provide side confinement to neurites (figure 3d). Specifically, for an optimized pillar diameter of 750 nm, the time GCs spent in periods of retraction is significantly reduced and that in the elongation phases increased as compared to flat PLL substrates. The larger lengths observed on these topographies is therefore the result of a growth dynamics privileging the growth phases versus the retraction phases.

3.1.3. Combination of adhesive and topographical constraints

Yamada et al. have achieved such a combination thanks to the in-mold patterning (iMP) technique: 5 µm high grooves were coated only at the level of their bottom surface, providing guiding tracks for axonal growth [64]. The iMP technique provides a dramatic gain in axon confinement efficiency as compared to adhesive or topographical constraints only, i.e., micro-printed PLL stripes and PLL-uniformly coated grooves (bottom and edge surfaces included), respectively. Interestingly, an important population of long (>1 mm) axons has elongated at 6 DIV inside grooves, a lesser one on iMP tracks and none on adhesive stripes. On all substrates, axons are predominantly found along the edges, a phenomenon called edge guidance [45], but in decreasing order of magnitude along grooves, iMP tracks and stripes. As the observed differences in length cannot be attributed to a difference in PLL-coating density (iMP substrates resulting from 2 PLL-transfer steps display a lower PLL surface density than micro-contact printed PLL stripes), one must conclude that providing vertical surface for GCs enhance edge effect and neurite growth velocity, an effect noticeable, although to a lesser extent, even if these edges are uncoated. It would be interesting at this point to observed GC behavior at high spatio-temporal resolution in both situations of coated and uncoated edges.

3.2. 3D confinement

Neurite confinement in 3D has recently been performed using sophisticated micro-fabrication techniques based on self-rolling of either thin SiNx [65] or InAlGaAs-based [66] strain-induced self-rolled-up nanomembranes. While it was not possible to follow the GC morphology inside the tube, Froeter et al. [65] reported a dramatic acceleration of mice cortical neuron elongation rate when crossing the tube (figure 3e).

Another way to implement 3D confinement is to use bulk hydrogel into which need to find their way and therefore undergo resistive forces distributed on their entire surface. The difficult task of following neuronal growth in collagen and halyuronic acid hydrogel was recently achieved by Santos et al. [59]. Here too, the velocity of neurons elongating in these 3D hydrogels is significantly higher than in control 2D conditions, as assessed by the length of hippocampal mice neurites [59] (figure 3f). In addition, neurites were more dynamic in 3D than in 2D: the speed, frequency, and length of extension and retraction events increased in the 3D condition. The molecular structure of fast

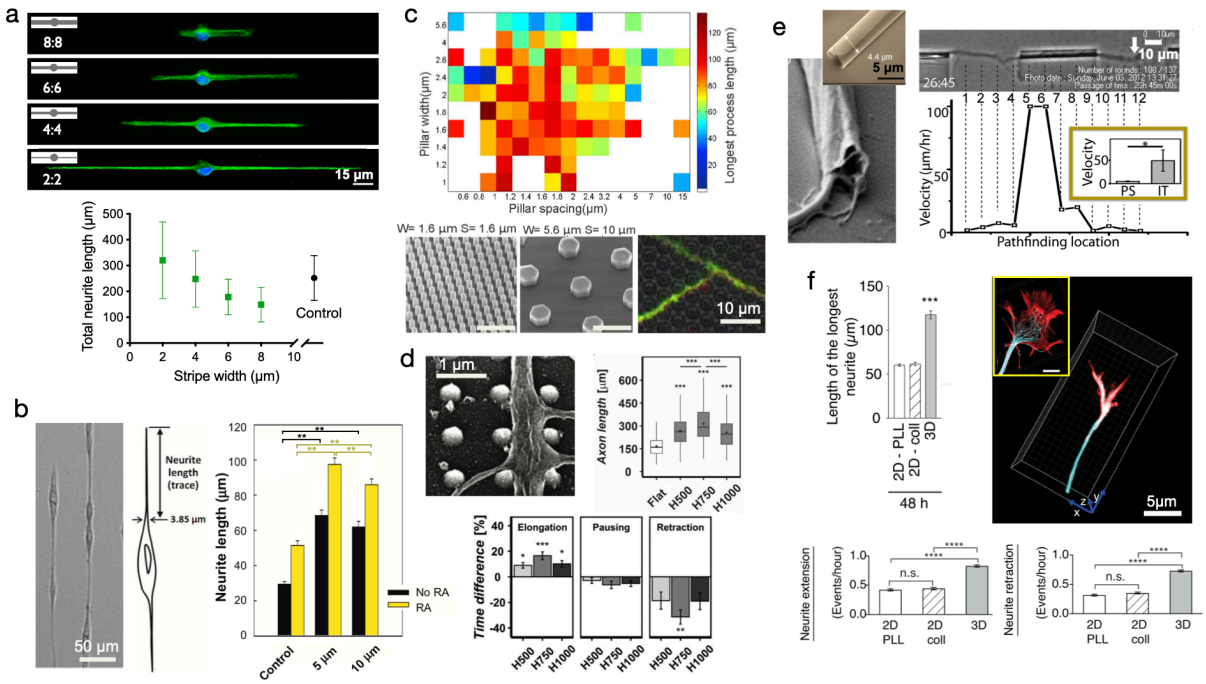

Figure 3 – **Increase of growth velocity induced by confinements of various dimensionality**
A-B: 1.5D confinement. A - Influence of the stripe width on the total neurite length after 3 days of culture: typical mouse hippocampal neuron morphologies and length distributions on simple stripe patterns. The control corresponds to a uniformly coated PLL coverslip. The patterning geometries used are sketched on each image. Adapted with permission from Tomba 2014 [56]. B – Influence of the stripe width on the extension of differentiated SH-SY5Y cell. Left: image of patterned SH-SY5Y cell on 10 µm collagen-I stripes on PLL-g-PEG back-filling. Middle: methodology of neurite length measurement, computed from where cell process shows a width of 3.85 µm and less to the tip. Right: graph of length distributions; Controls correspond to protein-unpatterned surfaces and retinoic acid (RA) activation or not (no RA); *: $p<0.01$. Adapted with permission from Poudel et al. (2013) [57].
C-D: 2.5D confinement. C – Surface plot of embryonic hippocampal axon length in function of width and spacing after 20 h (top) and illustrative images (bottom). Left and middle images: scanning electron microscopy (SEM) images of surfaces characterized by pillars of different width (w) and spacing (s); Values of w and s indicated above the images. Right image: axon confined in-between of w=1.8 µm and s=1.6 µm pillars; Axon (tau-1, green). D- SEM image of a cortical neuron growing in between 400 nm high, PLL coated pillars. Top graph: distribution of axon lengths at 3DIV. The numbers 500-750-1000 denote the pillar diameters (in nm). The pitch of each pillar array is twice of the pillar diameter. Bottom graph: percentage of time GCs spent elongating, pausing, and retracting normalized to the respective growth phases on the flat substrate. Adapted with permission from Milos et al. (2021) [62].
E-F: 3D confinement. E – Left: SEM images of microtubes, empty (top) or crossed by an axon (bottom). Right: a time-lapse phase contrast image of a cortical neuron show axonal pathfinding through a microtube. Key time-points of the growth cone trajectory are represented by vertical dashed lines (arrow: last position) toward the graph of velocities computed for each time-point. Inset: outgrowth velocity (µm/h) inside tube (IT) is significantly higher than that on planar substrate (PS); *:p = 0.05. Adapted with permission from Froeter et al. (2014) [65]. F – Top graph: length of the longest neurite in indicated conditions after 48 h; Bottom graphs: frequency of extension and retraction events of the DIC time lapse. Values are plotted as means ± SEM. ****$p < 0.0001$; ***$p < 0.001$; n.s., not significant. Images: STED images of immunolabeled GCs; Tubulin (Tuj 1, cyan) and actin (phalloidin, red). Adapted with permission from Santos et al. (2020) [59].

migrating 3D GCs is also markedly different from its more familiar 2D counterpart: microtubules reach the GC leading edge, compromising the usual 2D-associated GC partitioning into MT (central), acto-myosin (transition) and actin-rich (peripheral) domains. These recent and striking findings are in line with much earlier observation by Graves et al. on PC12 differentiated cells [67]. Very importantly, CNS neurons extend axons in 3D without exerting measurable pulling forces on their environment. Hippocampal neurons thus grow in an amoeboid mode when embedded in a soft 3D matrix [59].

In short, physico-chemical cues as different as adhesive contrast or topographical structures, as well as the mechanical resistance provided by a soft matrix all stimulate neuronal growth (and accelerate the axonal polarization process, although this aspect was not mentioned here). Is there a common mechanism supporting this generic output? To try to answer this question, I will review the elements provided by the literature regarding the key players driving neuronal growth at the sub-cellular and molecular scales.

4. Sub-cellular and molecular actors of the adaptive response to confinement

Most of the literature on GCs is based on the modalities of their interaction with adhesive and, in the vast majority of cases, planar substrates [**15**]. In this context, the stepwise iterative process of GC forward movement is based on a series of 4 steps (i.e., adhesive recognition, protrusion, engorgement and consolidation). Filopodia, the thin motile protrusions composed of tight parallel bundles of filamentous actin that emerge from the lamellipodial actin network of the central GC domain, are instrumental for the first two steps [see **13, 12** and **14** for reviews]. Filopodia respond to extracellular cues, acting as accurate sensors, alternating periods of extension and shortening. These dynamic changes in filopodia length are attributed to a balance between the rates of forward actin polymerization and myosin-driven actin retrograde flow, the latter being modulated by the establishment of adhesive contacts coupling the actin cytoskeleton to the substrate under the well accepted framework of clutching forces proposed by Chan and Odde [**68**]. Note that the transduction of retrograde F-actin flow into GC's forward movement by a modulation of F-actin-substrate coupling efficiency was already demonstrated in 1995 by Lin and Forscher in Aplysia GCs [**69**]. The average lifetime of a filopodium is modulated by adhesion, decreasing when the adhesion is not strong enough to transmit actomyosin activity onto the substrate in the form of traction forces [**54**]. An attenuated F-actin retrograde flow induced by a strengthening of adhesion clutch engagement promotes the entry of pioneer microtubules (MTs) into filopodia. This MT invasion is mediated by a random walk mechanism of microtubule plus end on minute timescales [**70**], stabilizing these protrusions, which results in a consolidated GC protruding activity. Specifically, the rate of the actin filament-bound microtubule rearward flow (~ 4.7−5 μm/min) is similar to that of F-actin (4.2–5.3 μm/min) in both vertebrate and invertebrate GCs [**14**]. Filopodia are also produced at the neurite level (and will be named neurite filopodia in the sequel, as opposed to GC filopodia), where they perform lateral sensing. The mechanisms of MT consolidation describe just above may lead in this case to collateral branching [**71**].

The various restriction or incentives to the extension of filopodia provided by confinement and changing environment modulate their characteristics. Nanometric ridge/groove pattern arrays as well as thin adhesive stripes on flat substrates reduce significantly the number of neurite filopodia [**72**][**39**] and their length [**72**]. In addition, Jang et al. observed two distinct populations of GC filopodia: a group of F-actin rich stabilized filopodia at the tip and a group of non-aligned, unstable filopodia on the distal part of the GC [**72**]. In general, the existence of an asymmetry in the spatial distribution and length of GC and neurite filopodia is well supported by the literature of neuronal growth in confined situations [**6**] [**73**][**60**][**61**][see also the short review of **74**]. On the microscopic point of view, the restricted angular range of the filopodia distribution along the direction of the tip motion is expected to bias the microtubule random walk, favouring their accelerated entry in filopodia. This process may favor a positive feedback loop: microtubules transport actin nucleators, promoting actin polymerization at the microtubule plus tips, which in turn guide microtubules. The well-described phenomenon of edge guidance could be considered as a direct consequence of this feedback loop. A mechanical view considering the force developed by these oriented filopodia would lead to the same conclusion, based on several reports stating a translocation and polymerization of microtubules towards the site of force application [**75, 24, 34**).

In composite adhesive-repellent substrates, the observed increase of neurite growth velocity when the anchoring points of GC filopodia are more distant from each other is more intriguing. The work of Senra et al., who found an inverse dependence between the filopodial length and the retrograde velocity, might constitute the beginning of an answer to the issue raised by such a fascinating observation [**76**]. If the opposite proposition would also be true, an increasing inter-dot distance would promote the production of long filopodia anchored at their edges. Turney et al. indeed reported the existence of such filopodia up to ~15 μm in length, partially invaded by MT, on non-adhesive portions between LN stripes, and a distribution of filopodia length skewed to larger lengths (i.e., up to ~25 μm) under the application of the Myosin II inhibitor blebbistatin [**54**]. Consistent with these findings, Ryu et al. proposed a saccade mode of growth, associated with remarkably spiky GCs

morphologies and filopodia bridging up to 10 µm Sema3F gaps separating adhesive dots [37]. Adhesive contact only at the tip of filopodia might be enough to allow their stabilization by invading MTs. In other terms, the retrograde actin flow might be sufficiently slow also on non-adhesive portions of the filopodia. Such a statement would however be in contradiction with the recent findings of Abe et al., who considered the configuration in which a filopodium extends over two surfaces of different adhesiveness [77]. More precisely, these authors measured distinct actin retrograde flows on the portions of the filopodium sitting either on PLL or LN substrates. Interestingly, this flow adjusts itself locally in response to the different adhesive strength of the substrates, with the portions on LN showing the expected lowest retrograde flow. What if now the traction forces exerted at the tip only would be enough to change the dynamics and density of MTs? This hypothesis is supported by the recent work of Vincentiis et al., who demonstrates an increased microtubule (MT) density and MT assembly upon the application of mechanical forces comparable to, or even lower [78] than the forces the GC itself can generate [34]. Dedicated experiments measuring the actin retrograde flow and the MT invasion on spiky GCs preparing for neurite extension in-between adhesive spots should help to solve such contradictions.
Even more intriguing is the behavior of GCs when the gap between adhesive spots increases over the typical mean filopodia length, reaching 30 µm. Ryu et al. observed a collapsed GC morphology soon after axon terminals left the PLL dots and moved on the Sema3F-printed region [37]. This morphology is conserved during an otherwise accelerated growth performed mostly on this molecular background, as expected from the low fraction of the surface occupied by PLL in this configuration. This GC morphology is not without reminding the one reported in 3D confinement which promotes, without adhesion and pulling on the hydrogel matrix, GC amoeboid (i.e., filopodia independent) migration at larger velocities as compared to flat substrate [59].

Overall, confinement-mediated enhanced growth rate seems to rely either on adhesive pulling forces in situations of adhesive or topographical constraints or, on the contrary, on expansive pushing forces in non adhesive 3D soft environments. Filopodia mediate the generation of tensile forces. Therefore, any change occurring in the orientation, length, or overall distribution of filopodia induced by the combination of lateral constraints with a relatively free and extensive space ahead of the GC will be instrumental for GC path finding and velocity. The mechanisms leading to amoeboid growth are unknown at this stage. However, it might be interesting to refer to the switch to fast amoeboid-like migration under conditions of low adhesion and strong confinement revealed by Liu et al., and in particular to the mode driven by weakly contractile protrusions [79]. Invading cells such as neurons could also employ amoeboid-based migration by adapting the cytoskeleton organization of their GCs. In-between these two extreme cases of migration modalities based on either pulling or pushing forces, the situation of collapsed but very motile GCs on poorly permissive substrates interspersed with highly adhesive areas [37] raises interesting questions about the possible occurrence of amoeboid-like locomotion in a wider range of experimental conditions.

5. About growth morphology and neurite elongation

The motion of GCs drives the elongation of axonal branches during development and regeneration. GCs are highly dynamic structures, capable of changing their morphology significantly over timescales as short as a minute. These two aspects are associated in the literature, in particular that devoted to in vivo studies dealing with the migration of e.g., commissural axons in various animal models (chicken [80], zebrafish [81]) or the migration of retinal neurons in mice [82]. Specifically, pauses are associated with GC enlargement and fast growth with elongated tapered forms. Interestingly, GCs exhibit spiking shapes prior to resuming their advance.
At this stage, I can raise the issue of the existence of a causal link between morphology and dynamics. This question has been partially addressed in vivo, with some attempts to find explanations for the observed GC morphologies. Specifically, Dumoulin et al. noticed that GCs of commissural axons squeezing their way in-between the densely packed non-neuronal cells populating the floor plate (FP) adopted elongated tapered forms associated with fast growth [54].

The same GCs slow down and spread at the exit of the FP, when encountering a zone of even denser packed glial processes [83]. However the complexity of nervous system tissues makes it difficult to reach definitive conclusions. In vitro systems are thus very useful to help unravel this complexity by preparing ad hoc substrates. Kim et al. reported accelerated hippocampal neuron growth on bacterial cellulose-based scaffolds associated with more elongated GC [84]. Different levels of confinement were also implemented in order to tune GC morphologies. In this line, Smirnov et al. [38] noticed that when a GC enters a node sitting on thin adhesive stripes, GCs both grew larger and slowed down, a behavior investigated in detail by [37]. This inverse correlation between GC size and velocity was also observed in *bag cell* neurons from the sea slug Aplysia californica cultured on PLL coated substrates [85]. These results, associated with the fact that the growth velocity increases when GCs are squeezed by any modality of confinement, establish clearly a causality between GC morphology and dynamics.

I have identified that the perception of the landscape of surface adhesiveness is operated by filopodia present along the neurites (lateral neurite filopodia) and around the GC (both laterally and longitudinally). When lateral sensing leads to a spreading of the neuronal structures, GC or neurite, a slowing down in the elongation rate occurs. In the opposite case of lateral size reduction, accelerated forward growth is observed. In the first case, GCs are somehow "depolarized", in contrast to the tapered "polarized" shapes associated with growth at higher velocity. Interestingly, the growth rate in the unconfined situation, when reported, lies somewhere in-between the extreme values reported in the entire range of geometrical constraints [56, see also the graph of figure 3a] [50] [37].

6. Open questions and perspectives

Cells, including neurons, spread out to the edges of adhesive micropatterns, increasing their surfaces by a factor of up to 10. Although this observation has been made numerous times, the questions it raises remain virtually ignored in the literature. Basically, such a spreading implies that (i) cells are able to transiently explore their environment on distances well beyond their spontaneous size, and (ii) when this exploration leads to the recognition of a frontier separating adhesive to non adhesive areas, the cell stably adjusts its perimeter to this boundary. What drives a cell to extend its surface a few times over the value it takes on a homogeneously coated surface remains a fascinating, unanswered question. A possible line of exploration would be the ability of filopodia to translate a discontinuity of adhesion along their lengths into various mechanisms responsible for cell spreading. I hope that such open questions will foster new experiments and theoretical developments.

GCs, as well as whole cells, spread on adhesive finite surfaces such as dots. How they regulate their length accordingly to their width for instance on stripes (in other terms, a surface which can be considered as infinite along one direction) has not been quantitatively addressed in details. It has however been reported that GCs can adjust their aspect ratio. Moreover, it appears quite clearly that the narrower the longer they are when confined laterally. This behavior is opposite to that of HeLa cells, which spread to a characteristic steady-state length that is independent of the pattern width [86]. Similarly, the migration speed under confinement of non-neuronal cells such as immune cells shows a decreasing trend in contrast to what is observed for the GC velocity [87]. As a result, neurites display longer lengths when restricted in their lateral spreading. The existence of a specialized, mechanosensitive structures, such as the GC at the neurite tip or propagative actin waves, seems therefore to confer on the neurons a unique way to establish and regulate their exceptional size.

Studies on neuron growth under confinement show that the compartmentalized structure of the GC needs to be reconsidered, at least partly, and with it the contribution of microtubules to its forward motion. This is particularly dramatic for axons growing inside 3D hydrogel, characterized by microtubule invasion of their very tip. Microtubule structure and dynamics inside GCs either confined (i.e., navigating on thin stripes, between pillars or within microchannels) or exploring non-adhesive substrates, both situations corresponding to an accelerated growth, have been relatively ignored compared to the actin cytoskeleton. The imaging of microtubules and of their partners (for instance

plus-end tracking proteins) eventually combined with traction force microscopy and micropatterning to reveal the force distribution inside confined GCs should contribute to refine theoretical models and decipher why confinement behaves as a spur for axonal growth.

Acknowledgments

The author warmly thanks all the PhD students who accompanied her with energy, relentless dedication and creativity in the field of in vitro neurosciences since 2007: Sophie Roth, Ghislain Bugnicourt, Céline Braïni, Renaud Renault, Josquin Courte, Claire Leclech, Mallory Dazza, Audric Jan and Teng Pan. A special thank to Caterina Tomba whose some of the results are included in this review. I also acknowledge the support of the Mission for transversal and interdisciplinary initiatives of the CNRS, program “défi Modélisation du Vivant”.

Bibliography

[1] Millet, L. J., & Gillette, M. U. (2012). Over a century of neuron culture: from the hanging drop to microfluidic devices. The Yale journal of biology and medicine, 85(4), 501.

[2] Chen, C. S., Mrksich, M., Huang, S., Whitesides, G. M., & Ingber, D. E. (1997). Geometric control of cell life and death. Science, 276(5317), 1425-1428.

[3] Wyart, C., Ybert, C., Bourdieu, L., Herr, C., Prinz, C., & Chatenay, D. (2002). Constrained synaptic connectivity in functional mammalian neuronal networks grown on patterned surfaces. Journal of neuroscience methods, 117(2), 123-131.

[4] Taylor, A. M., Blurton-Jones, M., Rhee, S. W., Cribbs, D. H., Cotman, C. W., & Jeon, N. L. (2005). A microfluidic culture platform for CNS axonal injury, regeneration and transport. Nature methods, 2(8), 599-605.

[5] Wyart, C., Cocco, S., Bourdieu, L., Léger, J. F., Herr, C., & Chatenay, D. (2005). Dynamics of excitatory synaptic components in sustained firing at low rates. Journal of neurophysiology, 93(6), 3370-3380.

[6] Clark, P., Britland, S., & Connolly, P. (1993). Growth cone guidance and neuron morphology on micropatterned laminin surfaces. Journal of cell science, 105(1), 203-212.

[7] Roth, S., Bugnicourt, G., Bisbal, M., Gory‐Fauré, S., Brocard, J., & Villard, C. (2012a). Neuronal Architectures with Axo-dendritic Polarity above Silicon Nanowires. Small, 8(5), 671-675.

[8] Paridaen, J. T., & Huttner, W. B. (2014). Neurogenesis during development of the vertebrate central nervous system. EMBO reports, 15(4), 351-364.

[9] Bak, M., & Fraser, S. E. (2003). Axon fasciculation and differences in midline kinetics between pioneer and follower axons within commissural fascicles.

[10] Tomba, C., & Villard, C. (2015). Brain cells and neuronal networks: Encounters with controlled microenvironments. Microelectronic Engineering, 132, 176-191.

[11] Omotade, O. F., Pollitt, S. L., & Zheng, J. Q. (2017). Actin-based growth cone motility and guidance. Molecular and Cellular Neuroscience, 84, 4-10

[12] Sánchez-Huertas, C., & Herrera, E. (2021). With the Permission of Microtubules: An Updated Overview on Microtubule Function During Axon Pathfinding. Frontiers in Molecular Neuroscience, 14.

[13] Dogterom, M., & Koenderink, G. H. (2019). Actin–microtubule crosstalk in cell biology. Nature Reviews Molecular Cell Biology, 20(1), 38-54.

[14] Pinto-Costa, R., & Sousa, M. M. (2021). Microtubules, actin and cytolinkers: how to connect cytoskeletons in the neuronal growth cone. Neuroscience Letters, 747, 135693.

[15] Lowery, L. A., & Vactor, D. V. (2009). The trip of the tip: understanding the growth cone machinery. Nature reviews Molecular cell biology, 10(5), 332-343.

[16] Polackwich, R. J., Koch, D., McAllister, R., Geller, H. M., & Urbach, J. S. (2015). Traction force and tension fluctuations in growing axons. Frontiers in Cellular Neuroscience, 9, 417.

[17] Lamoureux, P., Heidemann, S. R., Martzke, N. R., & Miller, K. E. (2010). Growth and elongation within and along the axon. Developmental neurobiology, 70(3), 135-149.

[18] Bernal, R., Melo, F., & Pullarkat, P. A. (2010). Drag force as a tool to test the active mechanical response of PC12 neurites. Biophysical journal, 98(4), 515-523.

[19] Bernal, R., Pullarkat, P. A., & Melo, F. (2007). Mechanical properties of axons. Physical review letters, 99(1), 018301.

[20] Anava, S., Greenbaum, A., Jacob, E. B., Hanein, Y., & Ayali, A. (2009). The regulative role of neurite mechanical tension in network development. Biophysical journal, 96(4), 1661-1670.

[21] Roth, S., Bisbal, M., Brocard, J., Bugnicourt, G., Saoudi, Y., Andrieux, A., ... & Villard, C. (2012b). How morphological constraints affect axonal polarity in mouse neurons. PloS one, 7(3), e33623.

[22] O'Toole, M., Lamoureux, P., & Miller, K. E. (2015). Measurement of subcellular force generation in neurons. Biophysical journal, 108(5), 1027-1037.

[23] Šmít, D., Fouquet, C., Pincet, F., Zapotocky, M., & Trembleau, A. (2017). Axon tension regulates fasciculation/defasciculation through the control of axon shaft zippering. Elife, 6, e19907.

[24] Kilinc, D., Blasiak, A., O'Mahony, J. J., & Lee, G. U. (2014). Low piconewton towing of CNS axons against diffusing and surface-bound repellents requires the inhibition of motor protein-associated pathways. Scientific reports, 4(1), 1-10.

[25] Franze, K. (2020). Integrating chemistry and mechanics: the forces driving axon growth. Annual review of cell and developmental biology, 36, 61-83.

[26] Xu, K., Zhong, G., & Zhuang, X. (2013). Actin, spectrin, and associated proteins form a periodic cytoskeletal structure in axons. Science, 339(6118), 452-456.

[27] Leterrier, C., Dubey, P., & Roy, S. (2017). The nano-architecture of the axonal cytoskeleton. Nature Reviews Neuroscience, 18(12), 713-726.

[28] Oliveri, H., & Goriely, A. (2022). Mathematical models of neuronal growth. Biomechanics and Modeling in Mechanobiology, 1-30.

[29] Ruthel, G., & Banker, G. (1998). Actin‐dependent anterograde movement of growth‐cone‐like structures along growing hippocampal axons: A novel form of axonal transport?. Cell motility and the cytoskeleton, 40(2), 160-173.

[30] Inagaki, N., & Katsuno, H. (2017). Actin waves: origin of cell polarization and migration?. Trends in cell biology, 27(7), 515-526.

[31] Braïni, C., Bugnicourt, G., & Villard, C. (2021). Neuronal growth from a volume perspective. Physical Biology, 18(1), 016007.

[32] Rossi, F., Gianola, S., & Corvetti, L. (2007). Regulation of intrinsic neuronal properties for axon growth and regeneration. Progress in neurobiology, 81(1), 1-28.

[33] Smith, D. H. (2009). Stretch growth of integrated axon tracts: extremes and exploitations. Progress in neurobiology, 89(3), 231-239.

[34] De Vincentiis, S., Falconieri, A., Mainardi, M., Cappello, V., Scribano, V., Bizzarri, R., ... & Raffa, V. (2020). Extremely low forces induce extreme axon growth. Journal of Neuroscience, 40(26), 4997-5007.

[35] Féréol, S., Fodil, R., Barnat, M., Georget, V., Milbreta, U., & Nothias, F. (2011). Micropatterned ECM substrates reveal complementary contribution of low and high affinity ligands to neurite outgrowth. Cytoskeleton, 68(7), 373-388.

[36] Zhao, S., Fan, W., Guo, X., Xue, L., Berninger, B., Salierno, M. J., & Del Campo, A. (2018). Microenvironments to study migration and somal translocation in cortical neurons. Biomaterials, 156, 238-247.

[37] Ryu, J. R., Kim, J. H., Cho, H. M., Jo, Y., Lee, B., Joo, S., ... & Sun, W. (2019). A monitoring system for axonal growth dynamics using micropatterns of permissive and Semaphorin 3F chemorepulsive signals. Lab on a Chip, 19(2), 291-305.

[38] Smirnov, M. S., Cabral, K. A., Geller, H. M., & Urbach, J. S. (2014). The effects of confinement on neuronal growth cone morphology and velocity. Biomaterials, 35(25), 6750-6757.

[39] Liu, W., Xing, S., Yuan, B., Zheng, W., & Jiang, X. (2013). Change of laminin density stimulates axon branching via growth cone myosin II-mediated adhesion. Integrative Biology, 5(10), 1244-1252.

[40] Natarajan, A., Smith, A. S., Berry, B., Lambert, S., Molnar, P., & Hickman, J. J. (2018). Temporal characterization of neuronal migration behavior on chemically patterned neuronal circuits in a defined in vitro environment. ACS Biomaterials Science & Engineering, 4(10), 3460-3470.

[41] Hardelauf, H., Waide, S., Sisnaiske, J., Jacob, P., Hausherr, V., Schöbel, N., ... & West, J. (2014). Micropatterning neuronal networks. Analyst, 139(13), 3256-3264.

[42] Tomba, C., Braïni, C., Wu, B., Gov, N. S., & Villard, C. (2014a). Tuning the adhesive geometry of neurons: length and polarity control. Soft matter, 10(14), 2381-2387.

[43] Tomba, C., Braïni, C., Bugnicourt, G., Cohen, F., Friedrich, B. M., Gov, N. S., & Villard, C. (2017). Geometrical determinants of neuronal actin waves. Frontiers in cellular neuroscience, 11, 86

[44] Kim, W. R., Jang, M. J., Joo, S., Sun, W., & Nam, Y. (2014). Surface-printed microdot array chips for the quantification of axonal collateral branching of a single neuron in vitro. Lab on a Chip, 14(4), 799-805.

[45] Renault, R., Durand, J. B., Viovy, J. L., & Villard, C. (2016). Asymmetric axonal edge guidance: a new paradigm for building oriented neuronal networks. Lab on a Chip, 16(12), 2188-2191.

[46] Forró, C., Thompson-Steckel, G., Weaver, S., Weydert, S., Ihle, S., Dermutz, H., ... & Vörös, J. (2018). Modular microstructure design to build neuronal networks of defined functional connectivity. Biosensors and Bioelectronics, 122, 75-87.

[47] Holloway, P. M., Hallinan, G. I., Hegde, M., Lane, S. I., Deinhardt, K., & West, J. (2019). Asymmetric confinement for defining outgrowth directionality. Lab on a Chip, 19(8), 1484-1489.

[48] Leclech, C., & Villard, C. (2020). Cellular and subcellular contact guidance on microfabricated substrates. Frontiers in Bioengineering and Biotechnology, 1198.

[49] Xing, S., Liu, W., Huang, Z., Chen, L., Sun, K., Han, D., ... & Jiang, X. (2010). Development of neurons on micropatterns reveals that growth cone responds to a sharp change of concentration of laminin. Electrophoresis, 31(18), 3144-3151

[50] Joo, S., Kang, K., & Nam, Y. (2015). In vitro neurite guidance effects induced by polylysine pinstripe micropatterns with polylysine background. Journal of biomedical materials research Part A, 103(8), 2731-2739

[51] Tomba, C., Migdal, C., Fuard, D., Villard, C., & Nicolas, A. (2022). Poly-l-lysine/Laminin Surface Coating Reverses Glial Cell Mechanosensitivity on Stiffness-Patterned Hydrogels. ACS Applied Bio Materials, 5(4), 1552-1563.

[52] Song, M., & Uhrich, K. E. (2007). Optimal micropattern dimensions enhance neurite outgrowth rates, lengths, and orientations. Annals of biomedical engineering, 35(10), 1812-1820.

[53] Chang, W. C., & Sretavan, D. W. (2008). Novel high-resolution micropatterning for neuron culture using polylysine adsorption on a cell repellant, plasma-polymerized background. Langmuir, 24(22), 13048-13057.

[54] Turney, S. G., Chandrasekar, I., Ahmed, M., Rioux, R. M., Whitesides, G. M., & Bridgman, P. C. (2020). Variation and selection in axon navigation through microtubule-dependent stepwise growth cone advance. bioRxiv.

[55] Kuhn, T. B., Schmidt, M. F., & Kater, S. B. (1995). Laminin and fibronectin guideposts signal sustained but opposite effects to passing GCs. Neuron, 14(2), 275-285.

[56] Tomba, C. (2014b). Primary brain cells in in vitro controlled microenvironments: single cell behaviors for collective functions (Doctoral dissertation, Université de Grenoble).

[57] Poudel, I., Lee, J. S., Tan, L., & Lim, J. Y. (2013). Micropatterning–retinoic acid co-control of neuronal cell morphology and neurite outgrowth. Acta Biomaterialia, 9(1), 4592-4598.

[58] Sun, Y., Huang, Z., Yang, K., Liu, W., Xie, Y., Yuan, B., ... & Jiang, X. (2011). Self-organizing circuit assembly through spatiotemporally coordinated neuronal migration within geometric constraints. PLoS One, 6(11), e28156.

[59] Santos, T. E., Schaffran, B., Broguière, N., Meyn, L., Zenobi-Wong, M., & Bradke, F. (2020). Axon growth of CNS neurons in three dimensions is amoeboid and independent of adhesions. Cell reports, 32(3), 107907.

[60] Lomboni, D. J., Steeves, A., Schock, S., Bonetti, L., De Nardo, L., & Variola, F. (2021). Compounded topographical and physicochemical cueing by micro-engineered chitosan substrates on rat dorsal root ganglion neurons and human mesenchymal stem cells. Soft Matter, 17(21), 5284-5302

[61] Wei, H., Chen, Z., Hu, Y., Cao, W., Ma, X., Zhang, C., ... & Chai, R. (2021). Topographically conductive butterfly wing substrates for directed spiral ganglion neuron growth. Small, 17(38), 2102062.

[62] Micholt, L., Gärtner, A., Prodanov, D., Braeken, D., Dotti, C. G., & Bartic, C. (2013). Substrate topography determines neuronal polarization and growth in vitro. PloS one, 8(6), e66170.

[62] Milos, F., Belu, A., Mayer, D., Maybeck, V., & Offenhäusser, A. (2021). Polymer nanopillars induce increased paxillin adhesion assembly and promote axon growth in primary cortical neurons. Advanced Biology, 5(2), 2000248.

[64] Yamada, A., Vignes, M., Bureau, C., Mamane, A., Venzac, B., Descroix, S., ... & Malaquin, L. (2016). In-mold patterning and actionable axo-somatic compartmentalization for on-chip neuron culture. Lab on a Chip, 16(11), 2059-2068.

[65] Froeter, P., Huang, Y., Cangellaris, O. V., Huang, W., Dent, E. W., Gillette, M. U., ... & Li, X. (2014). Toward intelligent synthetic neural circuits: directing and accelerating neuron cell growth by self-rolled-up silicon nitride microtube array. ACS nano, 8(11), 11108-11117.

[66] Koitmäe, A., Müller, M., Bausch, C. S., Harberts, J., Hansen, W., Loers, G., & Blick, R. H. (2018). Designer neural networks with embedded semiconductor microtube arrays. Langmuir, 34(4), 1528-1534.

[67] Graves, C. E., McAllister, R. G., Rosoff, W. J., & Urbach, J. S. (2009). Optical neuronal guidance in three-dimensional matrices. Journal of neuroscience methods, 179(2), 278-283.

[68] Chan, C. E., & Odde, D. J. (2008). Traction dynamics of filopodia on compliant substrates. Science, 322(5908), 1687-1691.

[69] Lin, C. H., & Forscher, P. (1995). Growth cone advance is inversely proportional to retrograde F-actin flow. Neuron, 14(4), 763-771.

[70] Fass, J. N., & Odde, D. J. (2003). Tensile force-dependent neurite elicitation via anti-β1 integrin antibody-coated magnetic beads. Biophysical journal, 85(1), 623-636.

[71] Gallo, G. (2011). The cytoskeletal and signaling mechanisms of axon collateral branching. Developmental neurobiology, 71(3), 201-220.

[72] Jang, K. J., Kim, M. S., Feltrin, D., Jeon, N. L., Suh, K. Y., & Pertz, O. (2010). Two distinct filopodia populations at the growth cone allow to sense nanotopographical extracellular matrix cues to guide neurite outgrowth. PloS one, 5(12), e15966.

[73] Mahoney, M. J., Chen, R. R., Tan, J., & Saltzman, W. M. (2005). The influence of microchannels on neurite growth and architecture. Biomaterials, 26(7), 771-778.

[74] Leclech, C., & Barakat, A. I. (2021). Is there a universal mechanism of cell alignment in response to substrate topography?. Cytoskeleton, 78(6), 284-292.

[75] Schaefer, A. W., Schoonderwoert, V. T. G., Ji, L., Mederios, N., Danuser, G., & Forscher, P. (2008). Coordination of actin filament and microtubule dynamics during neurite outgrowth. Developmental cell, 15(1), 146-162.

[76] Senra, D., Páez, A., Gueron, G., Bruno, L., & Guisoni, N. (2020). Following the footprints of variability during filopodial growth. European Biophysics Journal, 49(7), 643-659.

[77] Abe, K., Katsuno, H., Toriyama, M., Baba, K., Mori, T., Hakoshima, T., ... & Inagaki, N. (2018). Grip and slip of L1-CAM on adhesive substrates direct growth cone haptotaxis. Proceedings of the National Academy of Sciences, 115(11), 2764-2769.

[78] Albuschies, J., & Vogel, V. (2013). The role of filopodia in the recognition of nanotopographies. Scientific reports, 3(1), 1-9.

[79] Liu, Y. J., Le Berre, M., Lautenschlaeger, F., Maiuri, P., Callan-Jones, A., Heuzé, M., ... & Piel, M. (2015). Confinement and low adhesion induce fast amoeboid migration of slow mesenchymal cells. Cell, 160(4), 659-672.

[80] Dumoulin, A., Zuñiga, N. R., & Stoeckli, E. T. (2021). Axon guidance at the spinal cord midline—A live imaging perspective. Journal of Comparative Neurology, 529(10), 2517-2538.

[81] Andersen, S. S. (2021). Real time large scale $\textit {in vivo} $ observations by light-sheet microscopy reveal intrinsic synchrony, plasticity and growth cone dynamics of midline crossing axons at the ventral floor plate of the zebrafish spinal cord. arXiv preprint arXiv:2107.05242.

[82] Godement, P., Wang, L. C., & Mason, C. A. (1994). Retinal axon divergence in the optic chiasm: dynamics of growth cone behavior at the midline [published erratum appears in J Neurosci 1995 Mar; 15 (3): following table of contents]. Journal of Neuroscience, 14(11), 7024-7039.

[83] Lane, S., McDermott, K., Dockery, P., & Fraher, J. (2004). The developing cervical spinal ventral commissure of the rat: a highly controlled axon-glial system. Journal of neurocytology, 33(5), 489-501.

[84] Kim, D., Park, S., Jo, I., Kim, S. M., Kang, D. H., Cho, S. P., ... & Yoon, M. H. (2017). Multiscale modulation of nanocrystalline cellulose hydrogel via nanocarbon hybridization for 3D neuronal bilayer formation. Small, 13(26), 1700331.

[85] Ren, Y., & Suter, D. M. (2016). Increase in growth cone size correlates with decrease in neurite growth rate. Neural plasticity, 2016.

[86] Picone, R., Ren, X., Ivanovitch, K. D., Clarke, J. D., McKendry, R. A., & Baum, B. (2010). A polarised population of dynamic microtubules mediates homeostatic length control in animal cells. PLoS biology, 8(11), e1000542.

[87] Barbier, L., Sáez, P. J., Attia, R., Lennon-Duménil, A. M., Lavi, I., Piel, M., & Vargas, P. (2019). Myosin II activity is selectively needed for migration in highly confined microenvironments in mature dendritic cells. Frontiers in immunology, 10, 747.